

See discussions, stats, and author profiles for this publication at:  
<https://www.researchgate.net/publication/222691445>

# Hyperfine Structure in the Rotational Spectrum of GaF: A Comparison of Experimental and Calculated Spin–Rotation and Electric Field Gradient Tensors

ARTICLE *in* JOURNAL OF MOLECULAR SPECTROSCOPY · JANUARY 2001

Impact Factor: 1.48 · DOI: 10.1006/jmsp.2000.8211 · Source: PubMed

---

CITATIONS

22

---

READS

12

4 AUTHORS, INCLUDING:



[Roderick E. Wasylishen](#)

University of Alberta

401 PUBLICATIONS 6,583 CITATIONS

[SEE PROFILE](#)



[Corey James Evans](#)

University of Leicester

55 PUBLICATIONS 1,045 CITATIONS

[SEE PROFILE](#)

# Hyperfine Structure in the Rotational Spectrum of GaF: A Comparison of Experimental and Calculated Spin–Rotation and Electric Field Gradient Tensors

Roderick E. Wasylishen,<sup>\*,†,1</sup> David L. Bryce,<sup>\*</sup> Corey J. Evans,<sup>†</sup> and Michael C. L. Gerry<sup>†</sup>

<sup>\*</sup>Department of Chemistry, Dalhousie University, Halifax, Nova Scotia, Canada B3H 4J3; and <sup>†</sup>Department of Chemistry, University of British Columbia, 2036 Main Mall, Vancouver, British Columbia, Canada V6T 1Z1

Received May 19, 2000; in revised form July 27, 2000

The high-resolution pure rotational spectrum of GaF has been measured using a Balle–Flygare-type Fourier transform spectrometer. Improved nuclear quadrupolar coupling constants and rotational constants have been obtained along with the first reported fluorine spin–rotation constant for gallium fluoride,  $C_1(^{69}\text{Ga}^{19}\text{F}, \nu = 0) = +32.0(21)$  kHz. Accurate spin–rotation tensors from microwave or molecular beam spectroscopy are particularly important to NMR spectroscopists and theoreticians because these data provide information about anisotropic nuclear magnetic shielding in the absence of intermolecular effects. For quadrupolar nuclei such as gallium, the quadrupolar interaction is sufficiently large that it is very difficult to characterize shielding tensors directly via NMR spectroscopy. The experimentally determined nuclear quadrupolar coupling constants and spin–rotation constants for GaF are compared with the results of a series of high-level *ab initio* calculations carried out at various levels of theory with a range of basis sets. Further calculations on BF and AlF, supplemented with available experimental data for InF and TlF, allow for the investigation of trends in nuclear magnetic shielding, spin–rotation, and electric field gradient tensors in the group-13 fluorides. Calculations at the MP2/6-311++G\*\* and MP2/6-311G(2df, 2pd) levels provide the most consistently satisfactory results in comparison with the experimental data. © 2000 Academic Press

**Key Words:** gallium fluoride; hyperfine structure; rotational spectroscopy; group-13 fluorides; spin–rotation constants; quadrupolar coupling constants; electric field gradient tensors; *ab initio* calculations; nuclear magnetic shielding tensors.

## INTRODUCTION

The relationship between hyperfine parameters measured from high-resolution microwave spectroscopy and nuclear magnetic resonance (NMR) spectroscopy has been recognized for many years (1). Of particular interest in the present study is the relationship between the nuclear spin–rotation tensor and the nuclear magnetic shielding tensor. Accurate spin–rotation tensors gleaned from molecular beam or microwave spectroscopy are important because these data yield information on anisotropic nuclear magnetic shielding in the absence of intermolecular effects. In addition, for quadrupolar nuclei such as gallium, the quadrupolar interaction is sufficiently large that it is very challenging to characterize shielding tensors directly via NMR spectroscopy (2). Finally, accurate spin–rotation tensors provide critical tests of first-principles computational methods.

The purpose of this work is to present precise  $^{19}\text{F}$  and  $^{69/71}\text{Ga}$  nuclear spin–rotation data for gallium monofluoride, GaF, the simplest gallium halide. The experimental results will be compared with those obtained using high-level *ab initio* calculations and placed in the context of experimental results for the

other group-13 monofluorides and calculated results for BF and AlF. Experimental and calculated nuclear quadrupolar coupling constants will also be presented and discussed. Other recent theoretical efforts have been focused on the calculation of the total electronic energy and several spectroscopic properties of the lighter group-13 fluorides (3, 4).

There are two naturally occurring isotopes of gallium,  $^{69}\text{Ga}$  (natural abundance 60.108%) and  $^{71}\text{Ga}$  (natural abundance 39.892%), both with nuclear spin  $\frac{3}{2}$ . The nuclear quadrupole moments,  $Q$ , of these two isotopes have been reported recently by Pyykkö and co-workers as 173(3) and 109(2) mb, respectively (5). The magnetic moments of  $^{69}\text{Ga}$  and  $^{71}\text{Ga}$  are also of the same order of magnitude, 2.016589(44) and 2.562266(18) nuclear magnetons, respectively (6). Fluorine-19 has a natural abundance of 100%, a nuclear spin of  $\frac{1}{2}$  and a nuclear magnetic moment of 2.628868(8) nuclear magnetons (6). High-resolution microwave spectra of GaF were first reported by Hoeft *et al.* (7) in 1970. Nuclear quadrupolar coupling constants of  $-107.07(8)$  and  $-67.46(8)$  MHz were obtained for  $^{69}\text{Ga}$  and  $^{71}\text{Ga}$ , respectively, at the equilibrium structure. Also, values of the  $^{69}\text{Ga}$  and  $^{71}\text{Ga}$  nuclear spin–rotation constants were reported,  $+14(5)$  and  $+18(5)$  kHz, respectively. Subsequently, Honerjäger and Tischer (8) reported  $C_1(^{69}\text{Ga}) = 15.3(18)$  kHz. Hyperfine splittings due to  $^{19}\text{F}$  were not observed in either of the previous two investigations; therefore, information about the fluorine spin–rotation tensor has not been available. Accu-

<sup>1</sup> To whom correspondence should be addressed at Department of Chemistry, University of Alberta, Edmonton, Alberta, Canada T6G2G2. E-mail: Roderick.Wasylishen@ualberta.ca.

rate Dunham molecular parameters for GaF have been obtained from a millimeter-wave study of rotational transitions in the  $v = 0, 1$ , and 2 vibrational states (9). The equilibrium bond length reported from this study was 1.7743907(61) Å; the value obtained from analysis of vibrational–rotational spectra is 1.7743410(15) Å (10). Values of  $B_e$  and  $r_e$  are also available from an analysis of the  $C^1\Pi-X^1\Sigma^+$  system of GaF (11).

## EXPERIMENTAL AND COMPUTATIONAL PROCEDURES

### (i) Experimental

The pure rotational spectrum of GaF was measured using a Balle–Flygare-type Fourier transform spectrometer (12) that has been described in detail elsewhere (13). The spectrometer consists of a cavity formed by two spherical mirrors 28 cm in diameter and with a 38.4-cm radius of curvature, held approximately 30 cm apart. One mirror is fixed, while the other is used to tune the cavity to the microwave excitation frequency. A 4-mm-diameter glass rod coated with a layer of gallium was held near the center of the fixed mirror by a stainless steel nozzle cap 5 mm from the orifice of a General Valve series-9 pulsed nozzle (14). The gallium metal was ablated by the radiation from the second harmonic of a Nd:YAG laser (532 nm), in the presence of a 0.1%  $SF_6/Ne$  gas mixture (6 atm backing pressure), which was then expanded supersonically into the cavity via a 5-mm-diameter nozzle. This arrangement resulted in each line being split into two Doppler components, since the propagation of the microwave radiation was parallel to that of the supersonic jet. The use of such a parallel configuration results in improved sensitivity and resolution (13). The measurement accuracy is estimated to be better than  $\pm 2$  kHz at 22 GHz ( $\approx 0.1$  ppm). For well-resolved lines, the frequency was obtained by averaging the frequencies of the Doppler components in the frequency domain spectrum. For closely spaced or overlapped lines, the frequencies were obtained by fitting directly to the time domain signal to eliminate effects of lineshape distortion in the power spectrum (15). The strongest lines were easily seen in 20 averaging cycles. The rotational transition frequencies of both isotopomers of GaF were fitted using Pickett's exact fitting program, SPFIT (16).

### (ii) Computational

Quantum chemical calculations of electric field gradient (EFG) tensors were carried out at the following levels of theory using GAUSSIAN 98 (17): RHF (restricted Hartree–Fock), MP2 (second-order many-body perturbation (MP) theory), MP4SDQ (fourth-order MP theory with single, double, and quadruple excitations), CID (configuration interaction (CI) doubles), CISD (CI with singles and doubles), QCISD (CI with singles, doubles, and quadruples), CCD (coupled cluster doubles), and the B3LYP (18) implementation of density functional theory (DFT). GIAO (Gauge-Including Atomic Orbitals) (19) calculations of nuclear magnetic shielding tensors at the

RHF, MP2, and B3LYP levels of theory were also carried out with GAUSSIAN 98. The spin–rotation constant may be determined from the nuclear magnetic shielding tensor for a linear molecule (20) (*vide infra*). Nuclear  $g$  factors were taken from Ref. (6).

Multiconfigurational self-consistent field (MCSCF) calculations of the EFG tensors and spin–rotation constants for BF and AlF were carried out using the Dalton Quantum Chemistry Program (21). For these calculations, a restricted active space (RAS) wavefunction was used and the balanced active spaces were chosen based on the MP2 natural orbital occupation numbers (22). There are four orbital spaces which must be defined in these calculations: inactive, RAS1, RAS2, and RAS3. Our calculations allowed a maximum of two electrons to be excited from RAS1 and a maximum of two electrons to be excited into RAS3.  $C_{2v}$  symmetry is used in the calculations and thus there are four orbital symmetries:  $A_1$ ,  $B_2$ ,  $B_1$ ,  $A_2$ .

All calculations were done using a 43P Model 260 IBM RS/6000 workstation with dual 200-MHz processors. Basis sets were either available within the program libraries or obtained from the Extensible Computational Chemistry Environment Basis Set Database (23). All calculations were made using the following experimental equilibrium geometries:  $r_e$  ( $^{69}\text{GaF}$ ) = 1.7743410 Å (10);  $r_e$  ( $^{27}\text{AlF}$ ) = 1.654369 Å (7);  $r_e$  ( $^{11}\text{BF}$ ) = 1.262590 Å (24). First derivatives of the spin–rotation constants and quadrupolar coupling constants with respect to the bond length were estimated by calculating these properties at  $r_e + 0.01$  Å and  $r_e - 0.01$  Å.

The nuclear quadrupolar coupling constants ( $C_Q$ ) were determined from the calculated largest EFG component,  $eq_{zz}$ , by means of the following equation (25):  $C_Q = eq_{zz}Q/h$ . Conversion of  $eq_{zz}$  from atomic units to  $\text{Vm}^{-2}$  was effected by using the factor  $9.7177 \times 10^{21}$   $\text{Vm}^{-2}$  per atomic unit (6, 26). The following accepted values for  $Q$  were employed: 173 mb for  $^{69}\text{Ga}$  (5), 109 mb for  $^{71}\text{Ga}$  (5); 140.3 mb for  $^{27}\text{Al}$  (6); 40.59 mb for  $^{11}\text{B}$  (6).

## RESULTS

The  $^{69/71}\text{Ga}^{19}\text{F}$  molecule contains 40 electrons and the ground electronic state is  $^1\Sigma^+$ . The angular momenta coupling scheme used was  $\mathbf{I}_{\text{Ga}} + \mathbf{J} = \mathbf{F}_1$  and  $\mathbf{I}_{\text{F}} + \mathbf{F}_1 = \mathbf{F}$ , where  $\mathbf{J}$  is the rotational angular momentum, and  $\mathbf{I}_{\text{Ga}}$  and  $\mathbf{I}_{\text{F}}$  are the gallium and fluorine nuclear spin moments, respectively.

The  $J = 1 \leftarrow 0$  transition frequencies for the  $v = 0, 1$ , and 2 vibrational states of  $^{69}\text{Ga}^{19}\text{F}$  are given in Table 1. Similarly, the  $J = 1 \leftarrow 0$  transition frequencies for the  $v = 0$  and 1 states of  $^{71}\text{Ga}^{19}\text{F}$  are given in Table 2. A portion of the hyperfine structure of the  $J = 1 \leftarrow 0$  transition of  $^{69}\text{GaF}$  ( $v = 0$ ) is shown in Fig. 1. For GaF, the appropriate Hamiltonian may be expressed as

$$\mathcal{H} = \mathcal{H}_{\text{Rot}}(J, v) + \mathcal{H}_Q(\text{Ga}) + \mathcal{H}_{\text{SR}}(\text{Ga}) + \mathcal{H}_{\text{SR}}(\text{F}), \quad [1]$$

TABLE 1  
Measured Hyperfine Components of <sup>69</sup>GaF

	<i>J</i>	<i>F</i> <sub>1</sub> '	<i>F</i> '	<i>J</i> '	<i>F</i> <sub>1</sub> ''	<i>F</i> ''	Frequency / MHz	( <i>v</i> <sub>obs</sub> - <i>v</i> <sub>calc</sub> ) / kHz
<i>v</i> = 0	1	1.5	1	0	1.5	1	21448.9424	8.5
	1	1.5	2	0	1.5	2	21448.9424	-8.5
	1	2.5	2	0	1.5	1	21475.5932	-0.6
	1	2.5	3	0	1.5	2	21475.6328	0.6
	1	0.5	1	0	1.5	2	21496.8696	1.1
	1	0.5	0	0	1.5	1	21496.8888	-1.1
<i>v</i> = 1	1	1.5	1	0	1.5	1	21278.6540	8.5
	1	1.5	2	0	1.5	2	21278.6540	-8.5
	1	2.5	2	0	1.5	1	21305.0274	0.2
	1	2.5	3	0	1.5	2	21305.0655	-0.2
	1	0.5	1	0	1.5	2	21326.06	-19.3 <sup>a</sup>
	1	0.5	0	0	1.5	1	21326.06	-40.7 <sup>a</sup>
<i>v</i> = 2	1	1.5	1	0	1.5	1	21109.5802	8.9
	1	1.5	2	0	1.5	2	21109.5802	-8.9
	1	2.5	2	0	1.5	1	21135.6788	0
	1	2.5	3	0	1.5	2	21135.7188	0
	1	0.5	1	0	1.5	2	21156.5205	0
	1	0.5	0	0	1.5	1		0 <sup>b</sup>

<sup>a</sup> Taken from reference 7. The *v* = 1 <sup>69</sup>GaF line is overlapped by the *v* = 0 <sup>71</sup>GaF line. These lines were not included in the final fit.  
<sup>b</sup> Line not observed after 5000 averaging cycles.

where  $\mathcal{H}_{\text{rot}}(J, v)$  is the standard rotational term corrected for centrifugal distortion,  $\mathcal{H}_Q(\text{Ga})$  is the <sup>69</sup>Ga or <sup>71</sup>Ga nuclear quadrupolar coupling term, and  $\mathcal{H}_{\text{SR}}(\text{Ga})$  and  $\mathcal{H}_{\text{SR}}(\text{F})$  represent the nuclear spin-rotation interactions. The total hyperfine energy may thus be expressed as

$$E_{\text{hf}} = E_Q + E_{\text{SR}}(\text{Ga}) + E_{\text{SR}}(\text{F}), \tag{2}$$

where  $E_Q = -eQq Y(J, I, F)$  plus small second-order terms,

TABLE 2  
Measured Hyperfine Components of <sup>71</sup>GaF

	<i>J</i>	<i>F</i> <sub>1</sub> '	<i>F</i> '	<i>J</i> '	<i>F</i> <sub>1</sub> ''	<i>F</i> ''	Frequency / MHz	( <i>v</i> <sub>obs</sub> - <i>v</i> <sub>calc</sub> ) / kHz
<i>v</i> = 0	1	1.5	1	0	1.5	1	21326.3126	8.7
	1	1.5	2	0	1.5	2	21326.3126	-8.7
	1	2.5	2	0	1.5	1	21343.1226	-0.7
	1	2.5	3	0	1.5	2	21343.1633	0.7
	1	0.5	1	0	1.5	2	21356.4991	1.3
	1	0.5	0	0	1.5	1	21356.5182	-1.3
<i>v</i> = 1	1	1.5	1	0	1.5	1	21157.4938	8.6
	1	1.5	2	0	1.5	2	21157.4938	-8.6
	1	2.5	2	0	1.5	1	21174.1318	-0.4
	1	2.5	3	0	1.5	2	21174.1712	0.4
	1	0.5	1	0	1.5	2	21187.3686	0.8
	1	0.5	0	0	1.5	1	21187.3885	-0.8

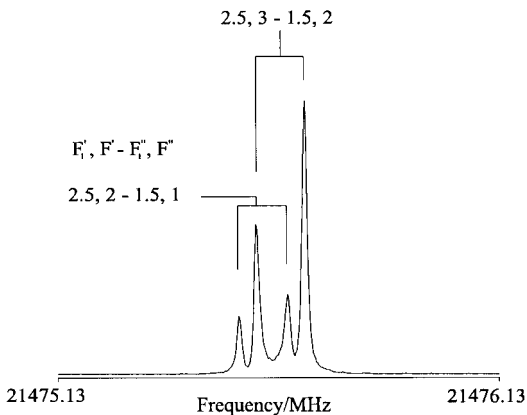


FIG. 1. A portion of the hyperfine structure of the *J* = 1–0 transition of <sup>69</sup>GaF in the *v* = 0 vibrational state. Experimental conditions: 0.3-μs pulse width; 0.1% SF<sub>6</sub> in Ne at 7 atm backing pressure; 25 averaging cycles; 8 K transform.

and  $E_{\text{SR}} = (C_I/2) [F(F + 1) - I(I + 1) - J(J + 1)]$ . Expressions for  $Y(J, I, F)$  are given in standard texts (27, 28). Although the Hamiltonian should in principle also contain both direct and indirect nuclear spin-spin coupling interactions (*Ia, c*, 29), these interactions are too small to perturb the spectra recorded here. In fact, interpolation of the results of recent high-level *ab initio* calculations in combination with available experimental data on the group-13 fluorides (29) indicate  $c_4(^{69}\text{GaF}) \approx -1.2$  kHz and  $c_3^{\text{indir}}(^{69}\text{GaF}) \approx +1.4$  kHz. From the known equilibrium internuclear separation and the latter indirect contribution,  $c_3$  is estimated to be approximately +4.4 kHz. Unfortunately, the spectral resolution is not adequate to determine these nuclear spin-spin coupling parameters conclusively. Incorporation of  $c_4$  into the fits only allows us to place an experimental maximum magnitude of -10 kHz on this parameter.

Molecular constants obtained for <sup>69</sup>GaF and <sup>71</sup>GaF are summarized in Tables 3 and 4. Equilibrium values of the rotational constant and the quadrupolar coupling constant are related to the values for a particular vibrational state in the following manner:

$$B_v = B_e - \alpha_e(v + \tfrac{1}{2}) + \gamma_e(v + \tfrac{1}{2})^2 \tag{3}$$

$$eQq_v = eQq_e + \alpha_{eQq}(v + \tfrac{1}{2}) + \gamma_{eQq}(v + \tfrac{1}{2})^2. \tag{4}$$

The equilibrium bond lengths determined by this procedure are 1.7743698(8) Å for <sup>69</sup>GaF and 1.7743697(9) Å for <sup>71</sup>GaF. These are also the same values as those of Hoeft and Nair (9), adjusted for differences in the values used for the fundamental constants.

Results of *ab initio* calculations of the gallium and fluorine spin-rotation constants and the gallium quadrupolar coupling constants for GaF are summarized in Tables 5–7 and 9–11

**TABLE 3**  
**Selected Molecular Properties for GaF for the First Few Vibrational Levels**

		$B_v$ / MHz	$D_v$ / kHz	$C_1(\text{Ga})$ / kHz	$C_1(^{19}\text{F})$ / kHz	$eQq/h$ / MHz
$^{69}\text{GaF}$	$v = 0$	10735.15953 (50)	14.3827 <sup>a</sup>	14.86 (56)	32.0 (21)	-106.5538 (61)
	$v = 1$	10649.90405 (60)	14.3518 <sup>a</sup>	14.86 <sup>b</sup>	32.0 <sup>b</sup>	-105.4411 (98)
	$v = 2$	10565.25831 (53)	14.3209 <sup>a</sup>	13.52 (60)	33.3 (24)	-104.3591 (65)
$^{71}\text{GaF}$	$v = 0$	10669.90795 (50)	14.2058 <sup>a</sup>	18.66 (56)	32.7 (21)	-67.1454 (61)
	$v = 1$	10585.42940 (50)	14.1773 <sup>a</sup>	18.71 (56)	32.1 (21)	-66.4542 (61)

<sup>a</sup> Fixed from reference 9.<sup>b</sup> Fixed to  $v = 0$  value.

along with corresponding calculations for the lighter group-13 fluorides, BF and AlF.

## DISCUSSION

### A. Nuclear Spin–Rotation Constants

#### (i) Gallium

For the  $^{69}\text{Ga}$  isotopomer of GaF, the  $v = 0$  gallium spin–rotation constant was determined to be 14.86(56) kHz. From the results summarized in Table 3, the ratio of the spin–rotation constants for the two gallium fluoride isotopomers in the ground vibrational state is  $C_1(^{71}\text{Ga})/C_1(^{69}\text{Ga}) = 1.256(60)$ . Within error, this value is equal to the ratio  $B(^{71}\text{GaF})g(^{71}\text{Ga})/B(^{69}\text{GaF})g(^{69}\text{Ga}) = 1.262871(29)$ . The gallium spin–rotation data presented here are in good agreement with previous work. Hoeft *et al.* reported values of  $C_1(^{69}\text{Ga}) = 14(5)$  kHz and  $C_1(^{71}\text{Ga}) = 18(5)$  kHz (7); Honerjäger and Tischer’s value for  $C_1(^{69}\text{Ga})$  in the  $v = 0$  state is 15.3(18) kHz (8). The present work has increased the precision of the gallium spin–rotation constant. This is the only gallium spin–rotation constant known with such high precision; however, values with relatively large errors have been reported for GaCl, 11(7) kHz (30), and GaI, 2.9(2.8) kHz (31).

Within experimental error, the gallium spin–rotation constant is identical for the first two vibrational levels, as evidenced by the  $^{71}\text{Ga}$  data in Table 3. However, the  $v = 2$  value for  $^{69}\text{GaF}$ , in conjunction with *ab initio* calculations of the derivative of the spin–rotation constant with respect to bond length ( $(\partial C_1/\partial r) < 0$ ), indicate that the spin–rotation constant at the equilibrium bond length should be slightly larger than the values for the  $v = 0$  and  $v = 1$  states.

(a) *Relationship between nuclear spin–rotation and nuclear magnetic shielding constants.* *Ab initio* calculations of the gallium and fluorine spin–rotation constants in GaF are summarized in Table 5. The following general discussion applies to both gallium and fluorine. For the majority of these calculations, the spin–rotation constant is not computed directly; rather it is determined from the calculated nuclear magnetic shielding tensor,  $\sigma$ . For a linear molecule such as GaF, the span ( $\Omega$ ) of the shielding tensor is usually given by  $\sigma_{\parallel} - \sigma_{\perp}$  (32), where  $\sigma_{\parallel}$  is the shielding experienced by the nucleus of interest when an applied magnetic field,  $B_0$ , is along the bond axis, and  $\sigma_{\perp}$  is the shielding experienced when  $B_0$  is perpendicular to the bond axis. We choose to relate the spin–rotation constant to the span because this parameter provides a measure of the anisotropy of the shielding tensor, a property of integral importance in most solid-state NMR experiments (33). The following relationship between the span of the shielding tensor and the spin–rotation tensor for a linear molecule is employed (1, 20):

$$C_1(r_e) = \frac{(\Omega - \Omega_p)(2mg_1B_e)}{m_p}. \quad [5]$$

Here,  $C_1(r_e)$  is the spin–rotation constant at the equilibrium bond length,  $m$  is the rest mass of an electron,  $g_1$  is the nuclear  $g$  factor ( $\gamma_1\hbar/\mu_N$ ),  $B_e$  is the rotational constant at the equilibrium bond length,  $m_p$  is the mass of a proton, and  $\Omega_p$  is a relatively small correction term known as the quadrupole term. In the case of a diatomic molecule,  $\Omega_p$  is proportional to the diamagnetic susceptibility of the neighboring atom and the inverse cube of the internuclear distance,  $\chi_{\text{atom}}^d r_e^{-3}$ . Interestingly,  $\Omega_p$  does not influence the isotropic chemical shielding

**TABLE 4**  
**Equilibrium Rotational Constants and Quadrupolar Coupling Constants for GaF**

	$B_e$ / MHz	$\alpha_e$ / MHz	$\gamma_e$ / MHz	$eQq_d/h$ / MHz	$\alpha_{eQq}$ / MHz	$\gamma_{eQq}$ / MHz
$^{69}\text{GaF}$	10778.0159(12)	85.8652(27)	0.30486(78)	-107.122(17)	1.143(36)	-0.015(11)
$^{71}\text{GaF}$	10712.37187(61)	85.07761(70)	0.29953 <sup>a</sup>	-67.4910(75)	0.6912(86)	-

<sup>a</sup> Fixed to value in reference 9.



**TABLE 5**  
***Ab Initio* Calculations of the Equilibrium Gallium and Fluorine Nuclear Magnetic Shielding Tensors in  $^{69}\text{GaF}$  and Derived Spin–Rotation Constants**

Method	Basis Set	$\Omega(^{69}\text{Ga})$ / ppm	$C_{\parallel}(^{69}\text{Ga})^a$ / kHz	$\sigma_{\text{iso}}(^{69}\text{Ga})$ / ppm	$C_{\parallel}(^{69}\text{Ga})^b$ / kHz	$\Omega(^{19}\text{F})$ / ppm	$C_{\parallel}(^{19}\text{F})^a$ / kHz	$\sigma_{\text{iso}}(^{19}\text{F})$ / ppm	$C_{\parallel}(^{19}\text{F})^b$ / kHz
RHF	6-311G*	826	12.9	2089	13.0	460	26.6	184	26.6
	6-311++G**	814	12.7	2097	12.8	408	23.4	218	23.4
	6-311G(2df,2pd)	807	12.6	2102	12.7	445	25.7	193	25.7
	cc-pVDZ	725	11.3	2155	11.4	449	25.9	191	25.9
	cc-pVTZ	751	11.7	2139	11.8	436	25.1	199	25.2
	cc-pVQZ	747	11.7	2142	11.8	414	23.8	213	23.8
MP2	6-311G*	929	14.5	2019	14.7	532	31.1	135	31.1
	6-311++G**	913	14.3	2029	14.4	464	26.9	180	27.0
	6-311G(2df,2pd)	900	14.1	2038	14.2	506	29.4	152	29.5
	cc-pVDZ	790	12.4	2112	12.5	503	29.2	154	29.4
	cc-pVTZ	834	13.1	2082	13.2	494	28.7	159	28.8
DFT / B3LYP	6-311G(2df,2pd)	1028	16.1	1954	16.2	608	35.8	84	35.8
expt. ( $\nu = 0$ ; this work)	-	-	14.86(56)	-	14.86(56)	-	32.0(21)	-	32.0(21)

<sup>a</sup> Calculated from the span using Eq. [5].

<sup>b</sup> Calculated from the isotropic nuclear magnetic shielding constant using Eq. [6].

constant, which is related to the spin–rotation constant by the equation:

$$C_{\parallel}(r_e) = - \frac{(3mg_{\text{I}}B_e)(\sigma_{\text{iso}} - \sigma_{\text{atom}}^d)}{m_p}. \quad [6]$$

The nonrelativistic free atom values,  $\sigma_{\text{atom}}^d$ , are taken from Ref. (34). It should be noted that the above expressions are valid only within the approximation developed by Flygare (20b, c). In Table 5, we present calculated spin–rotation constants (i) derived from Eq. [5] and (ii) derived from Eq. [6]. In general, spin–rotation data calculated from both equations provide very similar results. Since we are especially interested in the relationship between the span of the nuclear magnetic shielding tensor and the spin–rotation constant, we will discuss the results in terms of Eq. [5].

For gallium, the calculated results range from 11.3 kHz (RHF/cc-pVDZ) to 16.1 kHz (B3LYP/6-311G(2df, 2pd)); overall the agreement between experiment and theory is good. In particular the MP2 method with a moderately large basis set (6-311++G\*\* or 6-311G(2df, 2pd)) provides the most consistently satisfactory results for the calculations presented herein. The lack of electron correlation in the restricted Hartree–Fock (RHF) calculations results in a slight underestimation of the spin–rotation constant. Density-functional theory (DFT) overestimates the spin–rotation constant at the B3LYP/6-311G(2df, 2pd) level. It should be noted that the calculations are carried out at the equilibrium bond length, whereas

the reported experimental value of 14.86(56) kHz is for the ground vibrational state; consideration of the rovibrational effects on molecular properties for a series of diatomic molecules indicate that the corrections are typically less than 5% (29).

(b) *Comparison with known gallium magnetic shielding constants.* The span of the gallium shielding tensor in GaF, 900 ppm at the MP2/6-311G(2df, 2pd) level, and 949(35) ppm from the experimental spin–rotation constant ( $\nu = 0$ , calculated from Eq. [5]), represents more than 60% of the total known range of gallium shieldings ( $\sim 1400$  ppm, excluding gallium metal). To our knowledge, the gallium spin–rotation constant described here represents only the second quantitative experimental report of anisotropic gallium shielding. The first reported gallium shielding anisotropy was observed in a single-crystal  $^{71}\text{Ga}$  NMR study of the garnet  $\text{Y}_3\text{Ga}_5\text{O}_{12}$  ( $\Omega(\text{Ga(VI)}) = 38(9)$  ppm) (2b). Our calculated (nonrelativistic)  $^{69}\text{Ga}$  isotropic shielding (MP2/6-311G(2df, 2pd)) in GaF is 2038 ppm; a combination of the calculated value for  $\sigma_{\parallel}$  and our experimental span determined from the spin–rotation constant gives a value of 2005 ppm for  $\sigma_{\text{iso}}$ . Bühl has presented a series of gallium chemical shift calculations using the GIAO method at the SCF and MP2 levels (35). Based on the present calculations and those provided by Bühl, the GIAO/MP2 isotropic shielding of GaF is on the order of 100 ppm larger than that of aqueous  $\text{Ga}^{3+}$  (modeled as  $\text{Ga}(\text{H}_2\text{O})_6^{3+}$ ),  $\sigma_{\text{iso}} = 1930.4$  ppm, which is the  $^{69/71}\text{Ga}$  NMR chemical shift reference.

**TABLE 6**  
***Ab Initio* Calculations of the Equilibrium Boron and Fluorine Nuclear Magnetic Shielding Tensors**  
**in  $^{11}\text{BF}$  and Derived Spin-Rotation Constants**

Method	Basis Set	$\Omega(^{11}\text{B})$ / ppm	$C_I(^{11}\text{B})^a$ / kHz	$\sigma_{\text{iso}}(^{11}\text{B})$ / ppm	$C_I(^{11}\text{B})^b$ / kHz	$\Omega(^{19}\text{F})$ / ppm	$C_I(^{19}\text{F})^a$ / kHz	$\sigma_{\text{iso}}(^{19}\text{F})$ / ppm	$C_I(^{19}\text{F})^b$ / kHz
RHF	6-311G*	196	15.6	78.4	16.4	562	138	110	140
	6-311++G**	197	15.6	78.2	16.4	542	132	123	135
	6-311G(2df,2pd)	197	15.6	77.9	16.4	548	134	118	137
	cc-pVDZ	185	14.5	86.4	15.3	542	132	123	135
	cc-pVTZ	197	15.6	78.1	16.4	544	133	122	136
	cc-pVQZ	199	15.8	76.4	16.6	540	132	124	135
MP2	6-311G*	185	14.6	87.2	15.2	566	139	106	142
	6-311++G**	185	14.6	87.0	15.2	542	132	122	135
	6-311G(2df,2pd)	189	14.9	84.5	15.6	556	136	113	139
	cc-pVDZ	171	13.3	97.0	13.9	530	129	130	132
	cc-pVTZ	188	14.8	85.0	15.5	549	134	117	137
	cc-pVQZ	192	15.2	82.3	15.9	546	133	119	136
DFT / B3LYP	6-311G(2df,2pd)	207	16.5	72.8	17.1	602	148	83	151
RASSCF (2000/0000/ 3110/4331) <sup>c</sup>	cc-pV5Z	(direct)	15.6	(direct)	15.6	(direct)	127	(direct)	127
expt. ( $\nu = 0$ ) (ref. 36)	-	-	16.6(2)	-	16.6(2)	-	143(14)	-	143(14)

<sup>a</sup> Calculated from the span using Eq. [5].

<sup>b</sup> Calculated from the isotropic nuclear magnetic shielding constant using Eq. [6].

<sup>c</sup> Orbital spaces: inactive/RAS1/RAS2/RAS3.

(c) *Results for other group-13 fluorides: Putting the GaF data in context.* Shown in Tables 6 and 7 are the results of analogous calculations of the boron and aluminum nuclear magnetic shielding tensors and resulting spin-rotation constants for the lighter group-13 fluorides,  $^{11}\text{BF}$  and  $^{27}\text{AlF}$ . As the group-13 element is varied from boron to aluminum to gallium, the span of its shielding tensor increases from approximately 190 to 335 to 900 ppm.

For BF, the calculations at all levels provide boron spin-rotation constants which are within a few kilohertz of the experimental  $\nu = 0$  value of 16.6(2) kHz (36). Almost all of the calculated values are slightly less than the experimental result. It is important to note that the calculated derivative of the boron spin-rotation constant with respect to bond length is positive, indicating that 16.6(2) kHz is an upper limit on the experimental equilibrium  $^{11}\text{B}$  spin-rotation constant. Honerjäger and Tischer (37) have reported the aluminum spin-rotation constant in AlF ( $\nu = 0$ ) to be 8.2(13) kHz; our calculations reproduce this finding, with equilibrium values ranging from 7.17 kHz (RHF/cc-pVDZ) to 9.42 kHz (B3LYP/6-311G(2df, 2pd)). The only notable discrepancy between the use of Eq. [5] vs Eq. [6] arises here, for the aluminum spin-rotation constants determined from RHF and MP2 calculations with the 6-311G\* basis set and for the DFT calculation (Table

7). Apparently the 6-311G\* basis set is too small to reproduce accurately the isotropic magnetic shielding (RHF, MP2); the effect is a large overestimation of  $C_I(^{27}\text{Al})$ . It is not clear why the DFT/B3LYP method fails in this case, yet produces reasonable results for both BF and GaF.

Application of Eq. [5] (neglecting  $\Omega_\rho$ ) to the available experimental group-13 spin-rotation data for  $^{115}\text{InF}$  (38) ( $C_I(^{115}\text{InF}) = 17.47(10)$  kHz) and  $^{205}\text{TlF}$  (39) ( $C_I(^{205}\text{TlF}) = 126.03(12)$  kHz) indicates that the span of the indium shielding tensor in InF is  $\sim 1660$  ppm and the span of the thallium shielding tensor in TlF is  $\sim 5300$  ppm. Thus, although there is no trend in the spin-rotation constants for the group-13 elements in their diatomic fluorides (because of the dependence of this quantity on the nuclear magnetic moments of the relevant nuclei), the related quantity  $\Omega$  shows a distinct increase with increasing atomic number of the group-13 element. High-level *ab initio* calculations are presently out of reach in our laboratory (40) for the heavier group-13 fluorides, and indeed even if they were accessible, it should be pointed out that close agreement between experiment and the GIAO/MP2 level of theory is not expected owing to relativistic effects which are unaccounted for. In fact, even for gallium ( $Z = 31$ ), relativistic effects likely contribute to the experimentally determined values while our calculations do not incorporate relativistic

**TABLE 7**  
***Ab Initio* Calculations of the Equilibrium Aluminum and Fluorine Nuclear Magnetic Shielding Tensors in  $^{27}\text{AlF}$  and Derived Spin-Rotation Constants**

Method	Basis Set	$\Omega(^{27}\text{Al})$ / ppm	$C_1(^{27}\text{Al})^a$ / kHz	$\sigma_{\text{iso}}(^{27}\text{Al})$ / ppm	$C_1(^{27}\text{Al})^b$ / kHz	$\Omega(^{19}\text{F})$ / ppm	$C_1(^{19}\text{F})^a$ / kHz	$\sigma_{\text{iso}}(^{19}\text{F})$ / ppm	$C_1(^{19}\text{F})^b$ / kHz
RHF	6-311G*	330	8.44	308	19.0	411	36.2	213	36.7
	6-311++G**	325	8.31	575	8.46	373	32.7	237	33.2
	6-311G(2df,2pd)	323	8.26	577	8.42	416	36.7	209	37.2
	cc-pVDZ	282	7.17	604	7.32	412	36.3	212	36.8
	cc-pVTZ	318	8.14	580	8.29	400	35.2	219	35.8
	cc-pVQZ	297	7.58	594	7.74	385	33.8	230	34.3
MP2	6-311G*	342	8.76	300	19.3	443	39.3	190	39.9
	6-311++G**	336	8.60	569	8.72	394	34.6	223	35.3
	6-311G(2df,2pd)	335	8.57	569	8.70	445	39.5	189	40.2
	cc-pVDZ	292	7.44	598	7.57	435	38.6	195	39.2
	cc-pVTZ	328	8.39	573	8.54	426	37.7	202	38.3
DFT / B3LYP	6-311G(2df,2pd)	367	9.42	284	20.0	515	46.1	143	46.6
RASSCF (4110/0000/ 3110/6331) <sup>c</sup>	cc-pVQZ	(direct)	7.77	(direct)	7.77	(direct)	33.5	(direct)	33.5
expt. ( $\nu = 0$ ) (ref. 37)	-	-	8.2(13)	-	8.2(13)	-	d	-	d

<sup>a</sup> Calculated from the span using Eq. [5].

<sup>b</sup> Calculated from the isotropic nuclear magnetic shielding constant using Eq. [6].

<sup>c</sup> Orbital spaces: inactive/RAS1/RAS2/RAS3.

<sup>d</sup> Not observed in reference 37.

corrections. As an example of the effects of relativity on gallium nuclear magnetic shielding, we note that the absolute isotropic shielding constant for free  $\text{Ga}^{3+}$  is 2690 ppm if relativistic effects are ignored, and the relativistic value is 2855 ppm (41). In addition, the relationships between nuclear magnetic shielding and spin-rotation data as expressed by Eqs. [5] and [6] are not strictly valid when relativistic effects become important (42).

From the nuclear magnetic shielding theory of Ramsey (1a, c, 20a), it can be shown that the span, neglecting  $\Omega_p$ , is given for a diatomic molecule by

$$\Omega = \frac{e^2}{2m^2c^2} \left( \frac{\sum \langle o | L_x | k \rangle \langle k | L_x / r^3 | o \rangle + c.c.}{E_k - E_o} - \frac{Zm}{R} \right), \quad [7]$$

where  $R$  is the internuclear distance;  $Z$  is the atomic number of the atom bonded to the nucleus in question;  $|o\rangle$  and  $|k\rangle$  are ground and excited singlet states at energies  $E_o$  and  $E_k$ , respectively. Since for the group-13 fluorides the term in  $Z/R$  decreases from BF to TlF, the first term causes the major increase in  $\Omega$  for this sequence. Recent *ab initio* calculations strongly suggest a correlation between the Ga spans (and hence its shielding and spin-rotation constants) and the HOMO–LUMO gaps for GaH, GaF, GaCl, GaBr, and GaI (43). The

same correlations and trends hold for the aluminum and boron series (43, 44, 45). Recently reported indium spin-rotation constants for the indium halides InF, InCl, and InBr (38) reveal an increasing trend in the indium shielding tensor spans with increasing atomic number of the halogen. From the Flygare approach (Eq. [5]) without the quadrupole correction term, these values are  $\Omega(^{115}\text{InF}) = 1660$  ppm;  $\Omega(^{115}\text{In}^{35}\text{Cl}) = 2390$  ppm;  $\Omega(^{115}\text{In}^{79}\text{Br}) = 2760$  ppm. It should also be noted that although relativistic effects are not considered here, they are not likely to alter the qualitative trends in the properties of the group-13 halides.

#### (ii) Fluorine

The fluorine spin-rotation data, summarized in Table 3, indicate that the values of  $C_1(^{19}\text{F})$  for both the  $^{69}\text{Ga}$  and  $^{71}\text{Ga}$  isotopomers are the same within experimental error and are also essentially independent of vibrational state. These are the first fluorine spin-rotation constants reported for gallium fluoride. *Ab initio* calculations of the fluorine spin-rotation constant at the equilibrium bond length (Table 5) are in accord with the experimental result of  $\sim 32$  kHz. The results range from 23.4 kHz (RHF/6-311++G\*\*) to 35.8 kHz (B3LYP/6-311G(2df, 2pd)). As for the gallium calculations, the RHF and MP2 methods underestimate  $C_1$ , while the B3LYP/6-



TABLE 8

Summary of Experimental Fluorine Spin–Rotation Constants, Molecular Rotational Constants (56), and Fluorine Shielding Tensor Spans for Some Diatomic Fluorides

Molecule	$C_1(^{19}\text{F})/\text{kHz}$	$B_e/\text{MHz}$	$\Omega(^{19}\text{F})/\text{ppm}^a$	Ref.
$^{11}\text{BF}$	143	45477.03	549	36
$^{27}\text{AlF}$	40.2 <sup>b</sup>	16562.969 <sup>c</sup>	443	7
$^{69}\text{GaF}$	32	10778.0159	518	<sup>d</sup>
$^{115}\text{InF}$	18.3	7836.13502 <sup>c</sup>	419	38a
$^{205}\text{TlF}$	17.89	6690.13	467	39
$^{45}\text{ScF}$	58.7	11806.79620 <sup>c</sup>	868	57
$^{89}\text{YF}$	39.6	8683.6081 <sup>c</sup>	796	53
$\text{F}_2$	157	26687	1027	52
$\text{HF}$	284	628236	79	48
$^{35}\text{ClF}$	-22.67	15484.5	-256 <sup>32</sup>	46
$^{197}\text{AuF}$	-16.5	7924.83328	-364 <sup>32</sup>	47

<sup>a</sup> The span is calculated from the given spin-rotation constant and rotational constant using Eq. [5], but the quadrupole term,  $\Omega_p$ , has been neglected.

<sup>b</sup> Calculated value from the present work (MP2/6-311G(2df, 2pd)).

<sup>c</sup> The value of  $Y_{01}$  is reported.

<sup>d</sup> Present work.

<sup>e</sup> The value of  $B_0$  is reported.

311G(2df, 2pd) calculation overestimates it. Calculated derivatives of the fluorine spin–rotation constant with respect to bond length are positive, indicating that 32.0(21) kHz is an upper limit on the equilibrium value of  $C_1(^{19}\text{F})$  in  $^{69}\text{GaF}$ .

*Ab initio* calculations of the fluorine spin–rotation constants for the lighter group-13 fluorides,  $^{11}\text{BF}$  and  $^{27}\text{AlF}$ , are presented in Tables 6 and 7. Also shown are the calculated shielding tensor spans and isotropic shielding constants from which the spin–rotation constants were determined. The experimental  $v = 0$  value of the fluorine spin–rotation constant in  $^{11}\text{BF}$  is 143(14) kHz (36); both the RHF and MP2 calculations are in qualitative agreement with this value, but in general the experimental value is underestimated. An experimental fluorine spin–rotation constant for  $\text{AlF}$  has not been reported; however, given the good agreement between experimental data and the calculated data for  $\text{BF}$  and  $\text{GaF}$ , it is likely that  $C_1(^{19}\text{F})$  in  $\text{AlF}$  is on the order of 35–40 kHz.

(a) *Comparison with other diatomic fluorides.* Tabulated in Table 8 are the experimental fluorine spin–rotation constants, molecular rotational constants, and corresponding fluorine shielding tensor spans for the group-13 fluorides as well as for  $\text{HF}$ ,  $\text{F}_2$ ,  $\text{ClF}$ ,  $\text{AuF}$ , and the group-3 fluorides  $\text{ScF}$  and  $\text{YF}$ . The spans listed here have been determined based on Eq. [5], but neglecting the quadrupole term. This term is neglected for all results listed in this table for consistency because in the heavier diatomics, relativistic effects will likely play an impor-

tant role. The Flygare model itself does not consider the effects of relativity and thus inclusion of the small quadrupolar correction term is unnecessary for the present purpose. The data presented here are simply to illustrate the relative magnitudes of the fluorine shielding tensor spans for various diatomic molecules. For the group-13 fluorides, the  $^{19}\text{F}$  span is approximately constant at  $\sim 400$ – $500$  ppm as the group-13 element is changed. This observation is reproduced by the *ab initio* calculations for  $\text{BF}$ ,  $\text{AlF}$ , and  $\text{GaF}$ . As the data in Table 8 indicate, a value of  $\sim 500$  ppm for the fluorine shielding tensor span is approximately intermediate between the maximum known experimental value of greater than 1000 ppm for  $\text{F}_2$  and the “negative” (32) spans observed for molecules such as  $\text{ClF}$  (46) and  $\text{AuF}$  (47).

In discussing fluorine shielding anisotropies, it is useful to consider three classic cases, namely  $\text{HF}$ ,  $\text{F}_2$ , and  $\text{ClF}$ . The fluorine in hydrogen fluoride has one of the smallest shielding anisotropies, 79 ppm (48). The fluorine molecule and chlorine monofluoride are interesting in that their isotropic fluorine shieldings cover a large fraction of the total known shielding range:  $\sigma_{\text{iso}} = -232.8$  ppm for  $\text{F}_2(\text{g})$ , and  $+637.1$  ppm for  $\text{ClF}(\text{g})$  (49). This is intriguing since the atoms bonded to fluorine in these molecules are both halogens. The seemingly unusual shielding and negative span in  $\text{ClF}$  (also in  $\text{BrF}$  and  $\text{IF}$ ) is explained by a *positive* paramagnetic shielding term caused by a  $\sigma^* \leftarrow \pi^*$  excitation in an MO mostly on Cl (or Br or I) (50, 51). This is reflected in the negative fluorine spin–rotation constant,  $-22.67$  kHz (Table 8). Negative spin–rotation constants are uncommon but not unheard of; recent results show that both the gold and fluorine spin–rotation constants in  $\text{AuF}$ , for example, are negative (47). The large positive span and spin–rotation constant in  $\text{F}_2$  (52) may also be explained by consideration of the paramagnetic shielding term, which is large and negative (in  $\text{F}_2$  the  $\sigma^* \leftarrow \pi^*$  excitation found in  $\text{ClF}$  is forbidden by symmetry (50)). The fluorine spin–rotation constant for gallium fluoride reported here is of typical sign and magnitude for many diatomic fluorides. For example, in  $^{89}\text{YF}$ ,  $C_1(^{19}\text{F}) = 39.6$  kHz (53).

## B. Nuclear Quadrupolar Coupling Constants

The experimentally determined  $^{69/71}\text{Ga}$  quadrupolar coupling constants in  $\text{GaF}$  are presented in Tables 3 and 4. Both the rotational constants and the quadrupolar coupling constants for the first few vibrational states have been fitted to Eqs. [3] and [4] to obtain equilibrium values of  $eQq_e/h = -107.121(17)$  MHz and  $B_e = 10778.0159(12)$  MHz for the  $^{69}\text{GaF}$  isomer. These findings compare well with the previously determined values of Hoeft *et al.* ( $eQq_e/h = -106.53$  MHz;  $Y_{01} = 10778.023(8)$  MHz) (7), of Griffith *et al.* ( $B_e = 10778.80$  MHz) (11), of Hoeft and Nair ( $Y_{01} = 10778.0151(15)$  MHz) (9), and of Honerjäger and Tischer ( $eQq_{v=0}/h = -106.485(20)$  MHz) (8). The ratio  $eQq_e(^{71}\text{Ga})/eQq_e(^{69}\text{Ga})$  should be equal to the ratio of the

TABLE 9

*Ab Initio* Calculations of the Equilibrium Quadrupolar Coupling Constant for Gallium-69 in  $^{69}\text{GaF}$

Method	Basis Set	$eQq/h$ / MHz
RHF	6-311G*	-109.65
	6-311++G**	-108.29
	6-311G(2df,2pd)	-110.28
	cc-pVDZ	-85.59
	cc-pVTZ	-98.79
	cc-pVQZ	-97.22
MP2	6-311G*	-110.40
	6-311++G**	-108.80
	6-311G(2df,2pd)	-110.99
	cc-pVDZ	-85.69
	cc-pVTZ	-98.88
DFT/B3LYP	6-311G(2df,2pd)	-106.67
CISD	6-311G(2df,2pd)	-102.74
CCD	6-311G(2df,2pd)	-99.54
MP4SDQ	6-311G(2df,2pd)	-99.33
expt. (equilibrium; this work)	-	-107.121(17)

$^{71}\text{Ga}$  and  $^{69}\text{Ga}$  nuclear quadrupole moments reported by Tokman *et al.* (5), 0.630158(9); our experimental ratio, 0.630045(122), agrees within error.

Calculated values of the  $^{69}\text{Ga}$  nuclear quadrupolar coupling constants for GaF are presented in Table 9. Although the electric field gradient is a first-order property, high-level calculations are required to reproduce accurately experimental data (54). This is in part due to the fact that large basis sets must be employed to compensate for the poor description of the electronic density near the nucleus afforded by Gaussian-type orbitals (55). In general, the results in Table 9 are in good agreement with the experimental data, but not within experimental error. In particular, we note that for the molecules investigated here, the Pople-type basis sets (6-311G\*, 6-311++G\*\*, 6-311G(2df, 2pd)) seem to perform better than the correlation-consistent types (cc-pVXZ). The electron-correlated methods (MP2, DFT, CISD, CCD, MP4SDQ) do not provide systematically better results, at least with the basis sets used here. Employing Pople-type basis sets at the RHF or MP2 level yields a  $^{69}\text{Ga}$  nuclear quadrupolar coupling constant of approximately  $-109$  MHz.

The results of *ab initio* calculations of the  $^{11}\text{B}$  ( $I = \frac{3}{2}$ ) and  $^{27}\text{Al}$  ( $I = \frac{5}{2}$ ) quadrupolar coupling constants in BF and AlF (Tables 10 and 11) are presented for comparison with GaF. Experimental data have been reported for BF (36),  $eQq_{v=0}/h$  ( $^{11}\text{B}$ ) =  $-4.305(2)$  MHz; the calculations at the equilibrium bond length range from  $-3.62$  MHz (MP2/cc-pVDZ) to  $-5.15$

MHz (RHF/cc-pVQZ) and on the whole are in suitable accord with experiment. For AlF, the MP2/6-311G(2df, 2pd) value of  $-37.0$  MHz is in excellent agreement with the known experimental value for the equilibrium structure,  $-37.75(8)$  MHz (7). Both the quadrupolar coupling constant and the largest component of the EFG tensor (independent of  $Q$ ) increase as the atomic number of the group-13 element is increased. The trend continues with indium fluoride, for which the experimental  $^{115}\text{In}$  quadrupolar coupling constant is  $-723.795(12)$  MHz (38).

## CONCLUSIONS

The present work has provided a precise first value for the fluorine spin-rotation constant, improved the gallium spin-rotation constants, and slightly improved the rotational constants for gallium fluoride. Additionally, it has been demonstrated that calculations with sufficiently large basis sets at the MP2 level reproduce the experimentally determined spin-rotation constants for GaF, AlF, and BF. In general, the RHF and

TABLE 10

*Ab Initio* Calculations of the Equilibrium Quadrupolar Coupling Constant for Boron-11 in  $^{11}\text{BF}$

Method	Basis Set	$eQq/h$ / MHz
RHF	6-311G*	-4.85
	6-311++G**	-4.82
	6-311G(2df,2pd)	-5.13
	cc-pVDZ	-4.21
	cc-pVTZ	-5.08
	cc-pVQZ	-5.15
MP2	6-311G*	-4.30
	6-311++G**	-4.26
	6-311G(2df,2pd)	-4.59
	cc-pVDZ	-3.62
	cc-pVTZ	-4.52
	cc-pVQZ	-4.62
DFT/B3LYP	6-311G(2df,2pd)	-4.95
CID	6-311G(2df,2pd)	-4.76
CISD	6-311G(2df,2pd)	-4.73
QCISD	6-311G(2df,2pd)	-4.50
CCD	6-311G(2df,2pd)	-4.57
MP4SDQ	6-311G(2df,2pd)	-4.55
RASSCF (2000/0000/3110/4331)*	cc-pV5Z	-4.78
expt. ( $v = 0$ ) (ref. 36)	-	-4.305(2)

\* Orbital spaces: inactive/RAS1/RAS2/RAS3.

TABLE 11

***Ab Initio* Calculations of the Equilibrium Quadrupolar Coupling Constant for Aluminum-27 in  $^{27}\text{AlF}$** 

Method	Basis Set	$eQq/h$ /MHz
RHF	6-311G*	-39.4
	6-311++G**	-39.0
	6-311G(2df,2pd)	-39.6
	cc-pVDZ	-30.5
	cc-pVTZ	-39.7
	cc-pVQZ	-35.2
MP2	6-311G*	-37.1
	6-311++G**	-36.4
	6-311G(2df,2pd)	-37.0
	cc-pVDZ	-28.6
	cc-pVTZ	-37.0
DFT/B3LYP	6-311G(2df,2pd)	-37.8
CID	6-311G(2df,2pd)	-38.0
CISD	6-311G(2df,2pd)	-37.8
CCD	6-311G(2df,2pd)	-36.4
MP4SDQ	6-311G(2df,2pd)	-36.4
RASSCF (4110/0000/3110/6331) <sup>a</sup>	cc-pVQZ	-33.4
expt. (equilibrium, ref. 7)	-	-37.75(8)

<sup>a</sup> Orbital spaces: inactive/RAS1/RAS2/RAS3.

MP2 calculations tend to provide spin-rotation constants which are less than the experimental values, while the DFT calculations presented here overestimate the experimental values. Accurate quadrupolar coupling constants were obtained at the RHF level of theory, with little improvement resulting from the inclusion of electron correlation in the calculations.

**ACKNOWLEDGMENTS**

The authors thank the Natural Sciences and Engineering Research Council (NSERC) of Canada for research grants. We thank the members of the solid-state NMR group at Dalhousie University for helpful comments. D.L.B. thanks NSERC, the Izaak Walton Killam Trust, and Dalhousie University Faculty of Graduate Studies for postgraduate scholarships.

**REFERENCES**

- (a) N. F. Ramsey, "Molecular Beams," Oxford University Press, London, 1956; (b) W. H. Flygare, *Chem. Rev.* **74**, 653–687 (1974); (c) N. F. Ramsey, "Spectroscopy with Coherent Radiation: Selected Papers of Norman F. Ramsey with Commentary," World Scientific Series in 20th Century Physics, Vol. 21, World Scientific, Singapore, 1998; (d) W. Davies, "The Theory of the Electric and Magnetic Properties of Molecules" Wiley, London, 1967, pp. 201–204; (e) C. J. Jameson, in "Encyclopedia of Nuclear Magnetic Resonance" (D. M. Grant and R. K. Harris, Eds.), Wiley, Chichester, UK, 1996, pp. 1273–1281; (f) D. L. Bryce and R. E. Wasylshen, *J. Chem. Educ.*, in press.
- (a) J. Kodweiss, O. Lutz, W. Messner, K. R. Mohn, A. Nolle, B. Stüttz, and D. Zepf, *J. Magn. Reson.* **43**, 495–498 (1981); (b) T. Vosegaard, D. Massiot, N. Gautier, and H. J. Jakobsen, *Inorg. Chem.* **36**, 2446–2450 (1997); (c) T. Vosegaard, I. P. Byriel, L. Binet, D. Massiot, and H. J. Jakobsen, *J. Am. Chem. Soc.* **120**, 8184–8188 (1998); (d) D. Massiot, T. Vosegaard, N. Magneron, D. Trumeau, V. Montouillout, P. Berthet, T. Loiseau, and B. Bujoli, *Solid State Nucl. Magn. Reson.* **15**, 159–169 (1999).
- Y. Mochizuki and K. Tanaka, *Theor. Chem. Acc.* **101**, 257–261 (1999).
- J. Kobus, D. Moncrieff, and S. Wilson, *Mol. Phys.* **86**, 1315–1330 (1995).
- M. Tokman, D. Sundholm, and P. Pykkö, *Chem. Phys. Lett.* **291**, 414–418 (1998).
- I. Mills, T. Cvitaš, K. Homann, N. Kallay, K. Kuchitsu, "Quantities, Units and Symbols in Physical Chemistry," 2nd ed., Blackwell Science, Oxford, 1993.
- J. Hoeft, F. J. Lovas, E. Tiemann, and T. Törring, *Z. Naturforsch., A: Phys. Sci.* **25**, 1029–1035 (1970).
- R. Honerjäger and R. Tischer, *Z. Naturforsch., A: Phys. Sci.* **29**, 1919–1921 (1974).
- J. Hoeft and K. P. R. Nair, *Chem. Phys. Lett.* **215**, 371–374 (1993).
- J. F. Ogilvie, H. Uehara, and K. Horai, *J. Chem. Soc., Faraday Trans.* **91**, 3007–3013 (1995).
- W. B. Griffith, Jr., G. A. Bickel, H. D. McSwiney, and C. Weldon Mathews, *J. Mol. Spectrosc.* **104**, 343–346 (1984).
- T. J. Balle and W. H. Flygare, *Rev. Sci. Instrum.* **52**, 33–45 (1981).
- Y. Xu, W. Jäger, and M. C. L. Gerry, *J. Mol. Spectrosc.* **151**, 206–216 (1992).
- K. A. Walker and M. C. L. Gerry, *J. Mol. Spectrosc.* **182**, 178–183 (1997).
- J. Haekel and H. Mäder, *Z. Naturforsch., A: Phys. Sci.* **43**, 203–206 (1988).
- H. M. Pickett, *J. Mol. Spectrosc.* **148**, 371–377 (1991).
- M. J. Frisch, G. W. Trucks, H. B. Schlegel, G. E. Scuseria, M. A. Robb, J. R. Cheeseman, V. G. Zakrzewski, J. A. Montgomery, R. E. Stratmann, J. C. Burant, S. Dapprich, J. M. Millam, A. D. Daniels, K. N. Kudin, M. C. Strain, O. Farkas, J. Tomasi, V. Barone, M. Cossi, R. Cammi, B. Menonucci, C. Pomelli, C. Adamo, S. Clifford, J. Ochterski, G. A. Petersson, P. Y. Ayala, Q. Cui, K. Morokuma, D. K. Malick, A. D. Rabuck, K. Raghavachari, J. B. Foresman, J. Cioslowski, J. V. Ortiz, B. B. Stefanov, G. Liu, A. Liashenko, P. Piskorz, I. Komaromi, R. Gomperts, R. L. Martin, D. J. Fox, T. Keith, M. A. Al-Laham, C. Y. Peng, A. Nanayakkara, C. Gonzalez, M. Challacombe, P. M. W. Gill, B. G. Johnson, W. Chen, M. W. Wong, J. L. Andres, M. Head-Gordon, E. S. Replogle, and J. A. Pople, "GAUSSIAN 98, Revision A.4," Gaussian, Inc., Pittsburgh, PA, 1998.
- (a) A. D. Becke, *J. Chem. Phys.* **98**, 5648–5652 (1993); (b) C. Lee, W. Yang, R. G. Parr, *Phys. Rev. B* **37**, 785–789 (1988).
- (a) R. Ditchfield, *Mol. Phys.* **27**, 789–807 (1974); (b) K. Wolinski, J. F. Hinton, and P. Pulay, *J. Am. Chem. Soc.* **112**, 8251–8260 (1990).
- (a) N. F. Ramsey, *Phys. Rev.* **78**, 699–703 (1950); (b) W. H. Flygare, *J. Chem. Phys.* **41**, 793–800 (1964); (c) T. D. Gierke and W. H. Flygare, *J. Am. Chem. Soc.* **94**, 7277–7283 (1972).
- T. Helgaker, H. J. Aa. Jensen, P. Jørgensen, J. Olsen, K. Ruud, H. Ågren, T. Andersen, K. L. Bak, V. Bakken, O. Christiansen, P. Dahle, E. K. Dalskov, T. Enevoldsen, B. Fernandez, H. Heiberg, H. Hettema, D. Jonsson, S. Kirpekar, R. Kobayashi, H. Koch, K. V. Mikkelsen, P. Norman, M. J. Packer, T. Saue, P. R. Taylor, and O. Vahtras, "Dalton: An Electronic Structure Program, Release 1.0," 1997, <http://www.kjemi.uio.no/software/dalton/dalton.html>.
- (a) H. J. Aa. Jensen, P. Jørgensen, H. Ågren, and J. Olsen, *J. Chem. Phys.* **88**, 3834–3839 (1988); (b) J. Guilleme and J. S. Fabián, *J. Chem. Phys.* **109**, 8168–8181 (1998).
- [Basis sets were obtained from the Extensible Computational Chemistry

- Environment Basis Set Database (<http://www.emsl.pnl.gov:2080/forms/basisform.html>), as developed and distributed by the Molecular Science Computing Facility, Environmental and Molecular Sciences Laboratory, which is part of the Pacific Northwest Laboratory, P.O. Box 999, Richland, WA 99352, and funded by the U.S. Department of Energy. The Pacific Northwest Laboratory is a multiprogram laboratory operated by Battelle Memorial Institute for the U.S. Department of Energy under Contract DE-AC06-76RLO 1830. Contact David Feller or Karen Schuchardt for further information.]
24. F. J. Lovas and D. R. Johnson, *J. Chem. Phys.* **55**, 41–44 (1971).
  25. [We note that GAUSSIAN 98 provides EFG tensor components with signs opposite to the convention used here.]
  26. R. D. Brown and M. P. Head-Gordon, *Mol. Phys.* **61**, 1183–1191 (1987).
  27. W. Gordy and R. L. Cook, "Microwave Molecular Spectra," in "Techniques of Chemistry," (A. Weissberger, Ed.) Vol. XVII, Wiley, New York, 1984.
  28. C. H. Townes and A. L. Schawlow, "Microwave Spectroscopy," McGraw-Hill, New York, 1955.
  29. D. L. Bryce and R. E. Wasylshen, *J. Am. Chem. Soc.* **122**, 3197–3205 (2000).
  30. E. Tiemann, M. Grasshoff, and J. Hoeft, *Z. Naturforsch., A: Phys. Sci.* **27**, 753–755 (1972).
  31. K. P. R. Nair and J. Hoeft, *J. Mol. Spectrosc.* **85**, 301–313 (1981).
  32. [The span is more strictly defined as  $\Omega = \sigma_{33} - \sigma_{11} > 0$ ; see J. Mason, *Solid State Nucl. Magn. Reson.* **2**, 285–288 (1993). In the case of a diatomic molecule, this usually simplifies to  $\sigma_{\parallel} - \sigma_{\perp}$  (i.e.,  $\sigma_{\parallel} > \sigma_{\perp}$ ), but to adhere to the definition of the span being a positive quantity, the span for a diatomic molecule should be written strictly as  $|\sigma_{\parallel} - \sigma_{\perp}|$ . In the present work, when we refer to negative spans, this means that  $\sigma_{\parallel} < \sigma_{\perp}$ .]
  33. (a) C. J. Jameson and J. Mason, in "Multinuclear NMR," (J. Mason, Ed.), Chap. 3, (b) K. Schmidt-Rohr and H. W. Spiess, "Multidimensional Solid-State NMR and Polymers," Academic Press, San Diego, 1994, pp. 21–25.
  34. G. Malli and S. Fraga, *Theor. Chim. Acta (Berl.)* **5**, 275–283 (1966).
  35. M. Bühl, *Magn. Reson. Chem.* **34**, 782–790 (1996).
  36. G. Cazzoli, L. Cludi, C. Degli Esposti, and L. Dore, *J. Mol. Spectrosc.* **134**, 159–167 (1989).
  37. R. Honerjäger and R. Tischer, *Z. Naturforsch., A: Phys. Sci.* **29**, 342–345 (1974).
  38. (a) K. D. Hensel and M. C. L. Gerry, *J. Chem. Soc., Faraday Trans.* **93**, 1053–1059 (1997); (b) R. H. Hammerle, R. Van Ausdal, and J. C. Zorn, *J. Chem. Phys.* **57**, 4068–4070 (1972).
  39. R. V. Boeckh, G. Gräff, and R. Ley, *Z. Phys.* **179**, 285–313 (1964).
  40. Some *ab initio* calculations have been carried out for heavier group-13 halides. See for example: (a) D. Moncrieff, J. Kobus, and S. Wilson, *Mol. Phys.* **93**, 713–725 (1998); (b) C. W. Bauschlicher, Jr., *Chem. Phys. Lett.* **305**, 446–450 (1999).
  41. F. D. Feiock and W. R. Johnson, *Phys. Rev.* **187**, 39–50 (1969).
  42. P. Pyykkö, *Theor. Chem. Acc.* **103**, 214–216 (2000).
  43. (a) M. Gee and R. E. Wasylshen, in "Modeling NMR Chemical Shifts: Gaining Insights into Structure and Environment" (J. C. Facelli and A. C. de Dios, Eds.), ACS Symposium Series 732, American Chemical Society, Washington, DC, 1999, Chap. 19, (b) M. Gee and R. E. Wasylshen, unpublished manuscript.
  44. R. W. Schurko, R. E. Wasylshen, and H. Foerster, *J. Phys. Chem. A* **102**, 9750–9760 (1998).
  45. J. Gauss, U. Schneider, R. Ahlrichs, C. Dohmeier, and H. Schnöckel, *J. Am. Chem. Soc.* **115**, 2402–2408 (1993).
  46. R. E. Davis and J. S. Muentner, *J. Chem. Phys.* **57**, 2836–2838 (1972).
  47. C. J. Evans and M. C. L. Gerry, *J. Am. Chem. Soc.* **122**, 1560–1561 (2000).
  48. (a) D. K. Hindermann and C. D. Cornwell, *J. Chem. Phys.* **48**, 4148–4154 (1968); (b) W. H. Flygare, "Molecular Structure and Dynamics," p. 397, Prentice-Hall, Englewood Cliffs, NJ, 1978.
  49. C. J. Jameson, in "Multinuclear NMR" (J. Mason, Ed.), Chap. 16, Plenum Press, New York, 1987.
  50. (a) C. D. Cornwell, *J. Chem. Phys.* **44**, 874–880 (1966); (b) K. B. Wiberg, J. D. Hammer, K. W. Zilm, J. R. Cheeseman, and T. A. Keith, *J. Phys. Chem. A* **102**, 8766–8773 (1998).
  51. H. S. P. Müller and M. C. L. Gerry, *J. Chem. Phys.* **103**, 577–583 (1995).
  52. (a) M. R. Baker, C. H. Anderson, and N. F. Ramsey, *Phys. Rev. A: Gen. Phys.* **133**, 1533–1536 (1964); (b) I. Ozier, L. M. Crapo, J. W. Cederberg, and N. F. Ramsey, *Phys. Rev. Lett.* **13**, 482–484 (1964).
  53. K. A. Walker and M. C. L. Gerry, *J. Mol. Spectrosc.* **198**, 183–185 (1999).
  54. (a) L. Visscher, T. Enevoldsen, T. Saue, and J. Oddershede, *J. Chem. Phys.* **109**, 9677–9684 (1998); (b) G. B. Bacskay and A. D. Buckingham, *Mol. Phys.* **91**, 391–400 (1997).
  55. P. W. Atkins and R. S. Friedman, "Molecular Quantum Mechanics," 3rd ed., Oxford University Press, Oxford, 1997.
  56. (a) K. P. Huber and G. Herzberg, "Molecular Spectra and Molecular Structure: IV. Constants for Diatomic Molecules," Van Nostrand-Reinhold, New York, 1979; (b) NIST Chemistry Webbook, <http://webbook.nist.gov/chemistry> (accessed May 2000).
  57. W. Lin, S. A. Beaton, C. J. Evans, and M. C. L. Gerry, *J. Mol. Spectrosc.* **199**, 275–283 (2000).